Green synthesis of silver nanoparticles using *Eupatorium odoratum*against cell- wall anchored proteins (CWAPs) of Streptococcus mutans (gram positive bacteria) responsible for dental disorders in humans

ABSTRACT:

Aim: In the environmentally friendly manufacturing of silver nanoparticles, plant components like carbohydrates, lipids, enzymes, flavonoids, terpenoids, polyphenols, and alkaloids are employed as reducing agents. We aimed to green synthesize the silver nanopartciles (AgNPs) and study their effect on the expressive patterns of the cell wall anchored proteins in *S.mutans*.

Methods: Green synthesis of silver nanoparticles were done using *Eupatorium odoratum* leaf extract and were screened for antibacterial properties against *Streptococcus mutans* using UV-visible spectroscopy, scanning electron microscopy, X-ray diffraction and Fourier infrared spectroscopy.Further we studied the antibacterial activity of the AgNPs by well diffusion, MIC, Biofilm and gene expression studies.

Results: Utilizing optical inspection, it was found the nanoparticle production was successful when the yellow fluid turned brown.When compared to zone of inhibition (30mm) for the positive control at 50µg/ml, the zone of inhibition of the synthesised AgNPs was almost significantly similar (26mm) ($p<0.05$).The size of the silver nanoparticles (SNPs) produced in the current work ranged between 30 and 70nm and were biosynthesized utilising an aqueous extract of *E.odoratum*which acted as reducing agent.

Conclusion: The large-scale manufacture of NPs and the creation of biomedicines can be benefitted by this method of SNP synthesis that uses green chemistry.We conclude the potent antibacterial activity of the AgNPs synthesized at the molecular level.

Key words: Eupatorium odoratum, Silver nanoparticles, Antibacterial activity, S.mutans, Real time PCR.

INTRODUCTION:

The ability to create materials with superior chemical, electrical, thermal, mechanical, or optical qualities is what has made nanotechnology so appealing. Increased surface area, which increases chemical reactivity and mobility, is a characteristic of nanoscale materials. Some nanoparticles are employed as antibacterial and antifungal treatments because of their improved reactivity and suitably small size. Nanoparticles have the potential to be antibacterial through a variety of methods. The most prevalent antimicrobial action mechanisms have been identified as reactive oxygen species and nanoparticle adherence to microbial cells, as well as their penetration inside the cells [1].

UNDER PEER REVIEW

“AgNP synthesis using biological microorganisms or plant extracts has become a popular and straightforward substitute for chemical synthesis. The green synthesis process offers improvements over chemical methods because it is economical and environmentally benign. When compared to other biological procedures, the synthesis of AgNPs via plant extracts can be advantageous because it does not necessitate the upkeep of cell cultures and aseptic settings” [2]. There has been numerous research on the green production of AgNPs utilising plant extracts [3].

Eupatorium odoratum is used as an antibiotic, astringent, anti-rheumatic, and to treat stomach ulcers, diarrhoea, and headaches [4]. For many years, the genus Eupatorium has been recognised for its therapeutic benefits. Extracts of different species in *Eupatorium*have been found to contain a number of naturally occurring bioactive compounds, which appear to be a viable bioresource for lead compounds for novel medications and value-added goods. In various parts of the world, different *Eupatorium* species have been employed in conventional medicinal practises. Both *E. perfoliatum* and *E. purpureum*were used to cure rheumatism and influenza. Both preparations and essential oils of *Eupatorium* have demonstrated a range of intriguing biological activities, such as the antibacterial, cytotoxic, and virucidal properties displayed by *E. odoratum and E. salvia*[5].

The oral microbial biota of humans is an extremely varied biofilm. The human oral cavity is home to 25 species of oral streptococci, which account for 20% of all oral bacteria. These bacteria's taxonomy is intricate and unfinished. Oral streptococci have both allies and adversaries. Each species has evolved unique traits for competing with other species, colonising various oral areas due to continually changing environments and fending off external aggressions (host immune systemand other mechanical frictions). Oral disorders are caused by an imbalance in the local microbial biota, and in the right circumstances commensal streptococci can transform into opportunistic pathogens that cause disease in the host and harm to the host. The most significant microorganisms linked to the development of dental caries were described as belonging to the group of "mutans streptococci." *Streptococcus mutans* is the microbial species most significantly related with carious lesions, despite normally being in the human oral microbiome [6].

The complex biofilm population that makes up dental plaque is created as a result of bacteria adhering to dental surfaces [7]. Adhesion in *S. mutans* may be mediated by sucrose-dependent or -independent processes. *S. mutans* produces a number of surface adhesins that can bind to salivary substances, including those that contribute to the formation of the acquired pellicle on the teeth, when sucrose is absent.

One sortase from the SrtA subfamily is present in *S. mutans*[8]. “The chromosomal proximity of the SrtA subfamily members to the gyrA gene, which codes for DNA gyrase subunit A, is what first distinguishes them. Additionally, the genes that encode SrtA-type enzymes are never close to the genes that encode possible substrates. The cell surface protein P1 (also known as antigen I/II, SpaP, and Pac), fructanase (FruA), wall-associated protein A (WapA), wall-associated protein E (WapE), glucan-binding protein C (GbpC), and dextranase (DexA) are among the six proteins that the *S. mutans* UA159 genome encodes that contain the LPXTG motif located at the C terminus” [9].

Sortase's importance in the pathogenicity of various gram-positive pathogens has recently been discovered in *Streptococcus pneumoniae*, *Listeria monocytogenes*, and Staphylococcus aureus [10, 28-30]. A sortase mutant in *S. mutans* displayed a diminished capacity to colonise the teeth and oral mucosa.

Examining the inhibitory impact of manufactured AgNPs against *Streptococcus mutans*, which can be applied in the field of nanotechnology as a cost-effective, ecologically friendly, and secure technique, is therefore of utmost interest. Therefore, our goal is to create AgNPs from fresh *Eupatorium odoratum* leaf extract and test their antibacterial effectiveness against the pathogen *S. mutans*.

MATERIALS AND METHODS

Materials: In order to obtain biosynthesized AgNPs, fresh leaves of *Eupatorium odorata*were collected from local fields and stored before use at 4°C. The plant specimens were authenticated by Dr.Aruna, Plant biotechnologist, Reva University. We acquired silver nitrate ($AgNO_3$) from a HiMedia Ltd. *Streptococcus mutans* was procured from MTCC. Bacteria was grown in *Mitis salivarius* agar (MS) medium consisting of casein enzymatic hydrolysate (15.0 g/L), crystal violet (0.0008 g/L), Dextrose (1.0 g/L), Dipotassium phosphate (4.0 g/L), Peptic digest of animal tissue (5.0 g/L), Sucrose (50.0 g/L) and Trypan blue, 0.075 g/L without agar (pH 7.0).15g/L of agar was added to solidify the medium.

Extraction of the leaf samples: The preparation of the fresh leaves of *Eupatorium odorata* extract was done in accordance with a previously described process with a minor modification. Briefly, the leaves were cut into pieces after being properly cleaned with sterilised double deionized water (ddH2O). The cut components were then employed for extraction after being coarsely macerated using a blender. To 100ml of methanol, 20gm of slurry was added, and the mixture was shaken orbitally for 24 to 48 hours. The extract was filtered and concentrated using a rotary evaporator after incubation.

Green synthesis of AgNPs and their characterization: The effects of the amount of leaf extract were evaluated in the green synthesis of AgNPs in order to enhance the technique used to produce the metal nanoparticles. $AgNO_3$ (1mM) was dissolved in 100 ml of aqueous solution, and then methanolic leaf extract (50 mg/ml) was gradually added. It took around 24 hours of incubation before a colour shift could be seen. Control flasks with aqueous solutions of $AgNO_3$ and sterile ddH_2O were used to verify that the production of AgNPs was mediated by phytochemicals of *E.odorata* leaves. By shifting the optical hue to dark brown, the reduction of silver ions could then be seen. In order to analyse overnight samples of produced AgNPs, a UV-1800 Shimadzu Spectrophotometer was used (wavelength of 200-800 nm). The rapidly formed green synthesized AgNPs were obtained by centrifugation at 10,000 rpm for 10 min in a centrifuge machine (Remi, India) followed by carefully washed with sterile ddH_2O, freeze-dried and then stored at −80°C.The produced AgNPs were further characterised using a variety of techniques including NTA analysis, Fourier transform infrared

spectroscopy (FTIR; 450 and 4000 cm^{-1} with a resolution of 4 cm^{-1}), X-ray diffraction (XRD) and scanning electron microscopy, based on the quick reduction of AgNO3 into AgNPs (SEM).Scanning Electron microscopy (SEM) (SU8010, Hitachi, Japan) was used to characterize the shape of AgNPs.

***In vitro* Antibacterial Activity of synthesized AgNPs:** By using the agar well diffusion approach as reported by Elbeshehy *et al*. (2015) [11], the antimicrobial activity of produced AgNPs was assessed with minor modification. In a nutshell, 200*µ*l of bacterial culture that had been previously overnight-cultivated in MS broth at 37°C was poured into a Petri dish plate. This suspension had around 1x 10^8 CFU per ml. About 40*µ*l of AgNPs at final concentrations of 5, 10, 20, and 50*µ*g/ml were put onto agar wells at the same spacing (6 mm) and grew for 24 hours at 37 °C. Sterile distilled water was used as negative control. As a control, silver nanoparticles that weren't made with extract were employed. A positive control (Vancomycin 50*µ*g/ml) was also used in the study. The diameter of the zone of inhibition created around the centre of each sample was averaged to assess the antibacterial activity.

Minimum Inhibitory Concentration (MIC) of AgNPs: According to Panda et al., (2011) [12]the microdilution technique was used to estimate the MIC of the green synthesised AgNPs using 96 multi-well microtiter plates. The stock of AgNPs was added to the half-strength MS broth to modify the 5ml AgNPs solutions, resulting in final AgNP concentrations of 5, 10, 20 and 50µg/ml, respectively. *Streptococcus mutans* (10µl) at a concentration of around 1x 10^8 CFU/ml were added to solutions containing varied concentrations of AgNPs, while sterile ddH_2O served as the control (without AgNPs). After that, the samples were incubated for 12 hours at 37°C and 180 rpm. Positive testing was done using vancomycin (50µg/ml). For around 18 to 24 hours, the plates were incubated at 37°C. The MIC value was determined to be the lowest concentration at which turbidity seemed to be decreased. To calculate the MIC, the plates were examined for visible growth. Following incubation, the plates were checked for CFU/mL and their optical density was measured at 600nm using a PLATE reader (Genetix Ltd).

Biofilm Inhibition Assay: The 96-well microtitre plate technique reported by Masum *et al*. (2018) [13]was used to perform the AgNPs' inhibitions of bacterial biofilm formation, with a few minor modifications. To obtain the mid-exponential growth, the overnight cell suspension of *S. mutans* was re-cultured into a new MS broth at a shaker. Following that, sterile ddH2O was used as a reference and 10µl of bacterial cells (or around 1x 10^8 CFU/ml) were injected onto each well with AgNPs at a concentration of 50µg/ml. 24 hours of adhesion were allowed on the plates at 30°C without any agitation. The culture medium were then taken out of each well and carefully cleaned with sterile ddH_2O. The biofilm in the well of the plate was stained with a 100µl solution of crystal violet (CV, 0.1% w/v) at room temperature, which was then incubated for 45 minutes. Using a Genetix Microplate Spectrophotometer, the absorbance at 570 nm was measured after 125µl of acetic acid (33 percent, v/v) was used to dissolve the CV stain.

RNA extraction: The culture suspension was added to 50mL of MS medium and carefully mixed. AgNPs were added to tube labelled treatment in an amount of about 10**µ**l, and

vancomycin (50µg/ml) was added to the tube labelled positive control in an amount of about 10µl. Control tube is one that has not been treated. After adequately vortexing the mixture, it is incubated at 37°C for 24-48 hours. The cultures were taken out after incubation and utilised for the RNA extraction process. RNA extraction was carried in accordance with the manual's instructions. The cultures ($1x10^9$ bacteria) were centrifuged at 5000g for approximately 5 minutes at 4°C, and the resulting supernatant was discarded. 500µL of Buffer RLT were added to the pellet and vortexed violently for 5–10 seconds. The contents were then collected in a new tube after being centrifuged at full speed for approximately 10 seconds. By pipetting, an equivalent volume of 70% ethanol was added and properly mixed. A 2ml collection tube with an RNeasy spin column inside was loaded with around 700µL of the collected lysate. Following a 15-second centrifugation at a speed of around 9000g, the contents were removed. To clean the spin column, 700µL of Buffer RW1 was added to the column and centrifuged for 15 seconds at 9000g. After adding 500µL of buffer RPE to the RNeasy spin column, the flow-through was removed and the spin column washed for 15 seconds at 9000 g. The membrane was cleaned by repeating the previous process twice. A fresh collection tube was used to hold the column, and 30 to 50µL of RNase-free water were added. The RNA was then extracted from the mixture by centrifuging it for 1 minute at 9000 rpm and it was then kept at -20°C. The UV spectrophotometer was used to evaluate the RNA quality before it was utilised to synthesise complementary DNA (cDNA).

Reverse Transcription (RT) PCR: The RT-PCR kit and 200 U/L of SuperScriptTMII Reverse Transcriptase were used to create the cDNA (HiMedia). In a nutshell, the beginning reaction was initiated with approximately 2µg of the RNA acquired in the preceding phase. The amount of RNA that was collected was 1.98µg/ml. As a result, 1.12µL of the total RNA, 1µ L of RT enzyme and random primers were employed. The mixture was properly combined before being incubated at 25°C for 10 minutes. The generated cDNA was then kept in storage pending future usage for gene expression after 45 min of incubation at 70°C.

Real-time PCR: Primer 3 software was used to construct the primers for the real-time experiment (Table 1), which were then obtained from Sigma-Aldrich. Then, using the iQTM SYBR Green Supermix, the real-time PCR experiment was carried out in accordance with Malla Sudhakar *et al*(2020) [14]. (HiMedia). In the PCR experiment, the primers (600nM) and 1 L of the RT products were employed, and a total volume of 12.5 L was used for the reaction. To verify the positive amplification, each reaction was conducted in parallel with its corresponding negative control and in three copies.

Table No.1: List of primers used for Real time PCR (Lévesque CM, 2005).

Gene		**Primer sequence (5′ to 3′)**	Length of the primer	GC%	Tm	Product length
gyrA	FW	ATTGTTGCTCGGGCTCTTCCAG	22	55	65.8	252

	RV	ATGCGGCTTGTCAGGAGTAACC	22	55	71.2	
srtA	FW	GAAGCTTCCTGTAATTGGCG	21	60	65.4	
	RV	TTCATCGTTCCAGCACCATA	21	55	65.4	180
spaP	FW	TTTGCCGATGAAACGACCAC	21	58	62.34	
	RV	TACTCGCACTCCCTTGAGCCTC	22	58	62.3	324
fruA	FW	TGTAGGTCTCGGTTTGTGGGAC	22	60	58	
	RV	TCTTGAGCCAATGCTTCTGGTG	22	55	58.6	180
wapA	FW	TGACTTTGACTGATGTTGTCGGAG	24	55	56.8	
	RV	GAAAAATCCTCAGCATAAGGTCGC	24	55	56.8	205
wapE	FW	CTTCTGATAAAGCAACCGCCTAC	23	50	58	
	RV	AAGACCTAAGCCCATTCCAGTTC	23	55	58	215

Expression of gene members in samples: In the Corbett Research cycler, real-time quantification was done on the samples (both control and treatment) (Bio-Rad). The amplification programme used primers with a concentration of around 600nM for *srtA, spaP, fruA, wapA* and *wapE*. The programme was initially ran for roughly 40 cycles at 92°C for 50sec, 64°C for 45sec and with an elongation at 72°C for 50sec using about 1.12µl of the RNA products. In order to compare the mRNA expression, the housekeeping gene gyrA was amplified together with the relevant genes of interest. Using the $\Delta\Delta^{Ct}$ method, the relative amounts of mRNA in the test samples (including the control) were compared. The acquired Ct values for the desired gene were normalised to the housekeeping gene (gyrA).

Statistical analysis: Triplicates of each experiment were performed. The data was treated to two-way Analysis of Variance (ANOVA) when appropriate, and differences between samples were assessed using the Tukey's test ($p<0.05$). Analyses were conducted using the Microsoft Excel 2010 statistical programme throughout the investigation.

RESULTS and discussion

Synthesis and Characterization of the Synthesized Nanoparticles: In this investigation, multiple concentrations of *E. odoratum* leaf extract ranging from 2.5, 5, 10, and 15ml with 100ml of an aqueous solution of $AgNO_3$ (1mM) were examined in order to standardise the nanoparticles manufacturing technique. The quick shift in colour from light yellowish to dark brown after 120 minutes, induced by the breakdown of the 20 ml leaf fruit extract, showed that the amount of Ag+ in the $AgNO_3$ solution had been reduced to Ag^0.

Additionally, the findings of UV-visible spectrophotometers, which showed a spectrum of surface plasmon resonance (SRP) extending from 425 to 440nm of absorption band, validated the synthesis of AgNPs in the solution. In fact, a sharper and stronger absorption band at 435nm could be seen in the spectra of AgNPs made from the increased proportion

of leaf extract. Additionally, the UV-vis spectra (Fig.1) data revealed an increase in the reaction mixture's absorbance intensity over time, and the solution was stable after 24 hours of incubation, which suggests that the creation of nanoparticles in solution has finished.

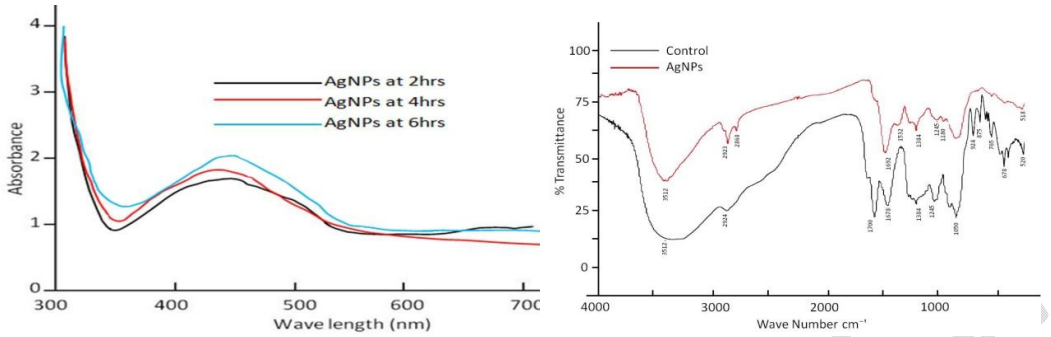

Fig.1: Image showing the UV-visible and FTIR spectra obtained for the synthesized AgNPs. Left: UV spectra; Right: FTRI spectra observed for the synthesized AgNPs.

FTIR spectra of synthesized AgNPs produced from *E. odoratum* extract following interaction with AgNO3 are displayed in Fig.1, together with extract control without $AgNO_3$. The C-C stretching vibration discovered the spectral peak at 1238 cm^{-1} in extract (shifted to 1180 cm^{-1} in AgNPs). In the case of synthesized AgNPs, a very strong absorption peak at 3512cm^{-1} that was pushed toward a lower wave number suggests that the silver ion (Ag^{+}) was bound to hydroxyl and/or amine groups in the *E. odoratum* leaf extract. The FTIR data shows a slight change in the peak in the spectra, as seen in Figure 1. The number of biological functional groups that serve as capping or stabilizing agents for nanoparticles is revealed by the spectrum analysis. Different absorption peaks were found in the FTIR analysis based on AgNPs mediated by the leaf extract at 3512, 2923, 2868, 1692, 1532, 1384, 1245, 1180, 1052, and 518 cm^{-1}. Additionally, the band at 1678 cm^{-1} in Leaf extraction was a result of the existence of amide I vibrations, and it was displaced to 1532 cm^{-1} in AgNPs as a result of the proteins that may have been connected to AgNPs by the amine groups.

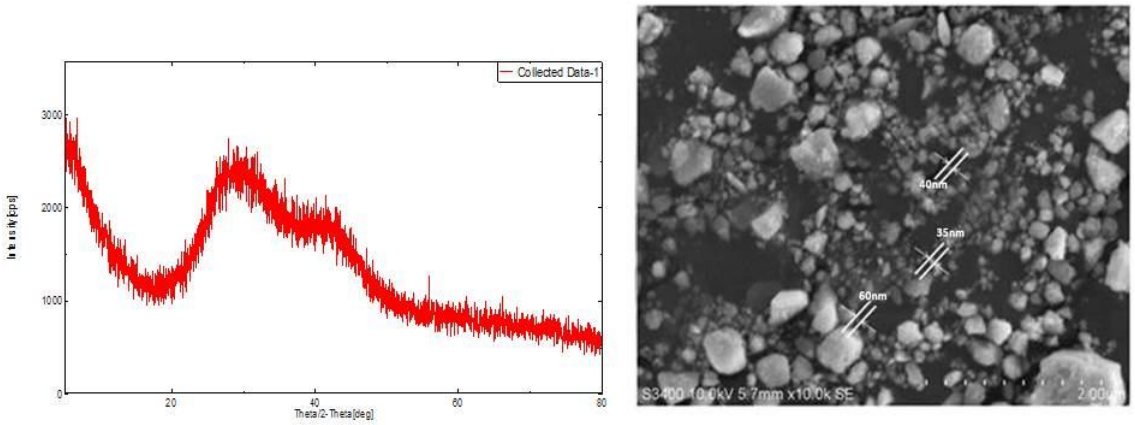

Fig.2**:** Image showing the XRD spectra and SEM images of synthesized AgNPs. Left: XD spectra. Right: HR-SEM analysis of synthesized AgNPs showing spherical shape and size of nanoparticles ranging between 30 – 60nm.

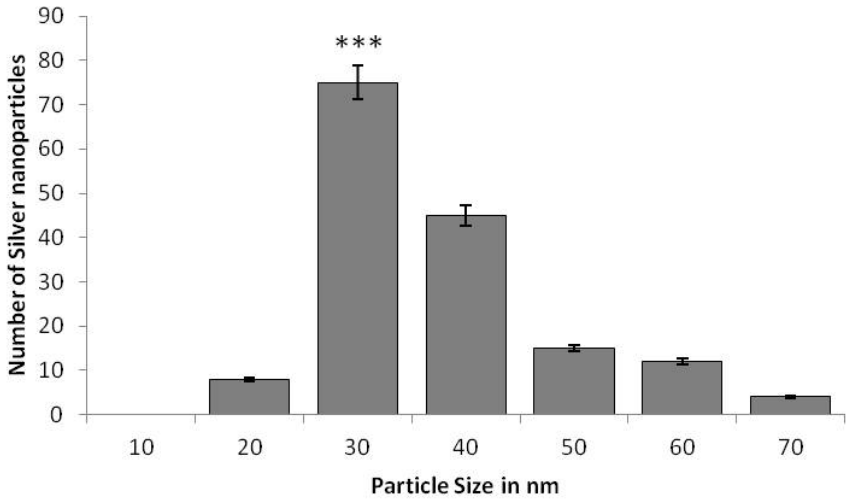

Fig.3: Graph showing the total size distribution of synthesized AgNPs as viewed from SEM. All the values are average of triplicates and expressed as number ±SD. *** Significant number observed ($p<0.05$).

For the detection of size of AgNPs nanopartcile tracking analysis (NTA) analysis by the Nano Sight (LM-20) was carried out (Fig. 3). The NTA images showed most of the synthesized nanoparticles are having an average size diameter of 35nm which was calculated on the basis of Brownian motion of particles (Fig.3). The size and shape of the produced AgNPs were investigated using SEM. The AgNPs were primarily scattered and more or less spherical in form. The particles ranged in size from 20 to 70nm (Fig. 3). XRD results indicate that the synthesized particles are face-centred round structures of silver (Fig. 2).

***In vitro* Antibacterial Activity of synthesized AgNPs:** The biosynthesized AgNPs demonstrated good sensitivity responsiveness against *S. mutans* at the four different doses after 24 hours of incubation in the MS agar media compared to Positive and control. The inhibitory zone width increased with increasing AgNPs concentrations (5–50 g/ml) against strain *S. mutans*. The largest inhibitory zone was created by AgNPs at a concentration of 50µg/ml, followed by AgNPs at a concentration of 5µg/ml. In contrast, untreated control AgNPs demonstrated an inhibitory zone of 2 and 6mm at concentrations of 5µg/ml and 50µg/ml, respectively (Fig.4). When compared to the inhibition zone of 30mm for the positive control at 50µg/ml, the zone of inhibition of the synthesised AgNPs was almost significantly similar (26mm) ($p<0.05$).The synthesised AgNPs demonstrated exceptional antibacterial effect against strain *S. mutans*, according to the data as a whole.

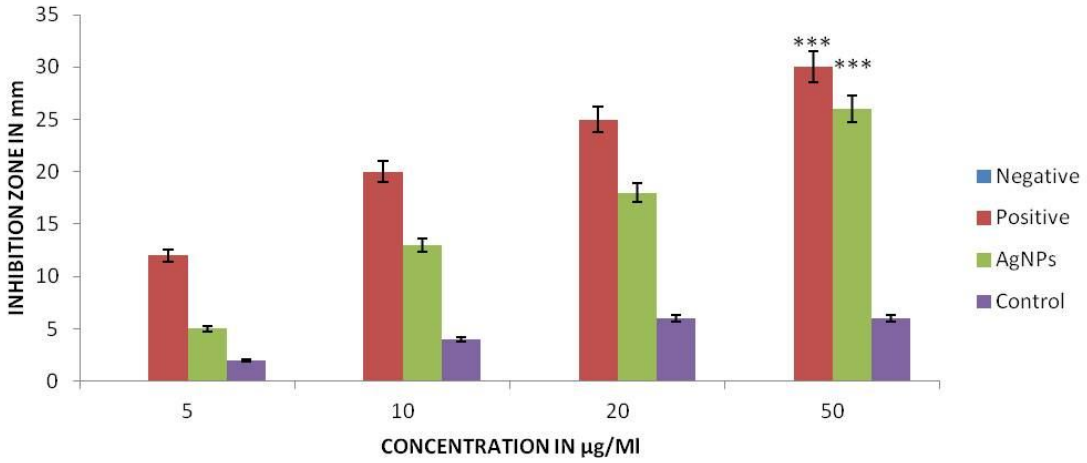

Fig.4: Graph showing the Invitro inhibitory effect of synthesized AgNPs by *E.odoratum* against *Streptococcus mutans*. All the values are average of triplicates and values are represented as value ±S.D. *** represents the significance of data remembered at $P<0.05$.

MIC of synthesized AgNPs: The findings of this investigation demonstrated that after 12 hours of incubation, AgNPs exhibited a discernible antibacterial activity against *S. mutans* in comparison to both positive control and the control (Fig.6). Distinct amounts of AgNPs had different antibacterial effects. In general, OD_{600} values decreased from 1.11 to 0.14 at 50µg/ml for AgNPs when compared to positive control (0.08) at similar concentration **(Fig.5)**. The control AgNPs without treatment do showed activity but was significantly less with OD of 0.61 at 50µg/ml. A two way ANOVA was done to compare the significance between the

samples and the concentrations. Significant effect was seen both within the samples and between the concentrations [F (4,8) = 0.365527, p = 0.000381] and [F(2,8)= 0.12266, p=0.022125].

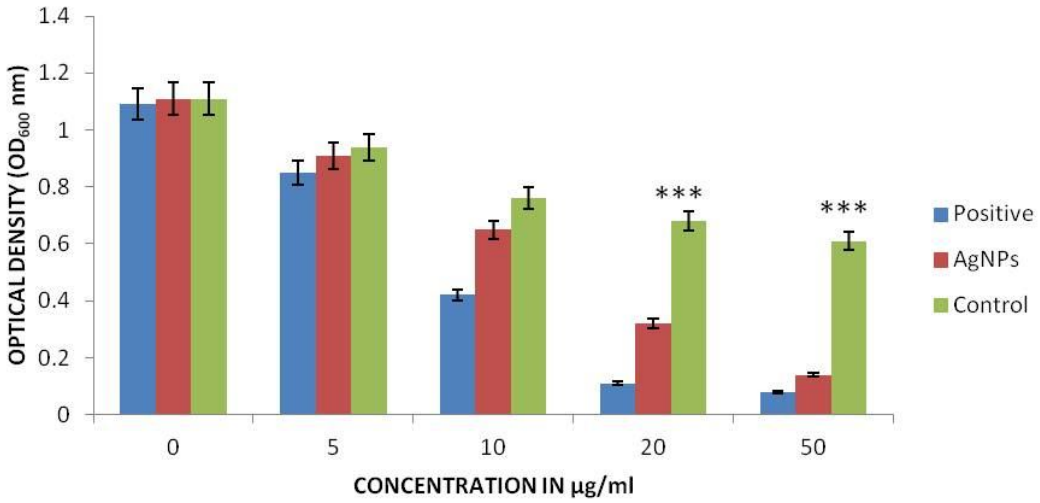

Fig.5: Graph showing the inhibition of growth by AgNPs mediated by *E.odoratum* leaf extract against *S.mutans*. All the values are average of triplicates and values are represented as value ±S.D. *** represents the significance of data remembered at P<0.05.

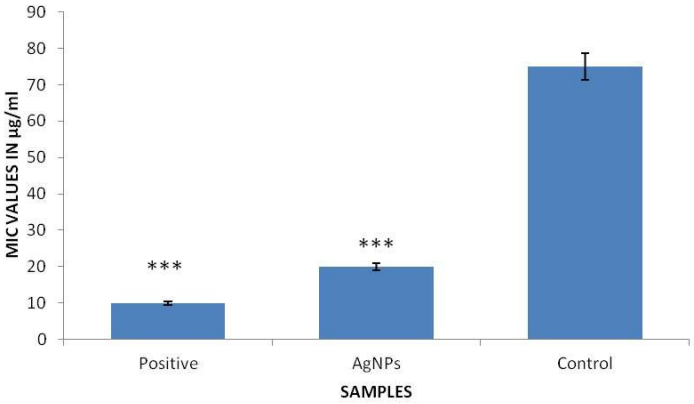

Fig.6: Graph showing the MIC values of AgNPs mediated by *E.odoratum* leaf extract against *S.mutans*. All the values are average of triplicates and values are represented as value ±S.D. *** represents the significance of data remembered at P<0.05.

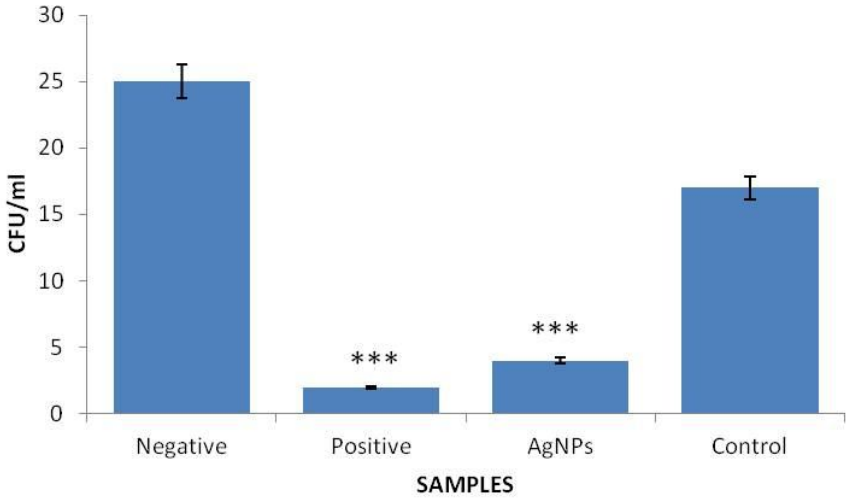

Fig.7: Graph showing the CFU/ml values of the AgNPs mediated by *E.odoratum* leaf extract against *S.mutans*. All the values are average of triplicates and values are represented as value ±S.D. *** represents the significance of data remembered at P<0.05.

MIC values greater than 50 were not considered in the study (control MIC was >75). MIC values were found to be 10 and 20 for positive control and green synthesized nanoparticles. The values were significant between the samples remembered are P<0.05. CFU were reported to be 2 and 4 positive control and green synthesized nanoparticles. The control nanoparticles without treatment showed about 17 CFU/ml which was not as significant as the synthesized AgNPs. These results are in accordance with the agar well diffusion method in the previous section.

Biofilm inhibition assay: The biofilm inhibition assay was found to be highly significant in terms of positive control and the control. Though, it was time dependant the effect was significantly seen in the synthesized AgNPs when compared to control. The results were in accordance to disc diffusion study. A two-way ANOVA between the treatments and time period was conducted to compare the effect of biofilm inhibition of the extracts. All effects were statistically significant at the 0.05 significance level. There was a significant effect between the control and synthesized AgNPs remembered at the p<0.05 level [F (2,4) = 0.248711, p = 0.006289]. *Post hoc* comparisons using the Tukey HSD test indicated that the mean score for the control was significantly different from positive control and AgNPs.Indeed, the OD_{595} value of control was 0.76 without treatment, while the synthesized AgNPs had a lower

OD_{595} value (0.12) at 24 hour incubation. Positive control on the other hand showed an OD_{595} value of 0.02**(**Fig.8**)**.

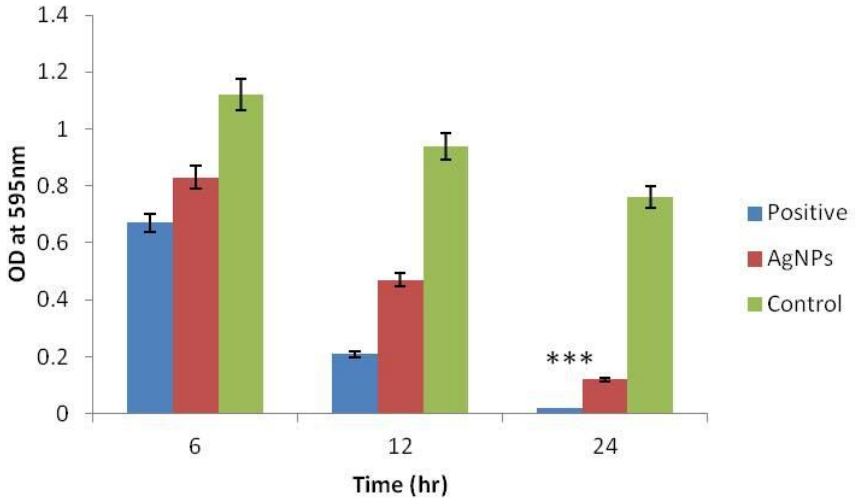

Fig. 8: Graph showing the biofilm inhibition values of the AgNPs mediated by *E.odoratum* leaf extract against *S.mutans* at different time periods (6, 12 and 24hr). All the values are average of triplicates and values are represented as value ±S.D. *** represents the significance of data remembered at P<0.05.

Expression of gene members in samples: All the gene members were found to be positively correlated to the treatment and responded with under expression. The results were consistent in both positive and treatment. All the gene members were found to be significantly underexpressed when compared to the control and positive control ($P < 0.05$). Expression levels of *wapA* were found to be reduced to 0.94 fold from 7.65 fold expression by the control. Positive control expression was found to be 0.21 when compared to 7.65 (control). Similarly the expression was found to be 1.15, 2.13, 0.78 and 1.54 respectively for srtA, spaP, fruA and wapE gene members. Positive control was found to be negatively regulated (-1.54) for srtA gene member (Fig.9**)**.

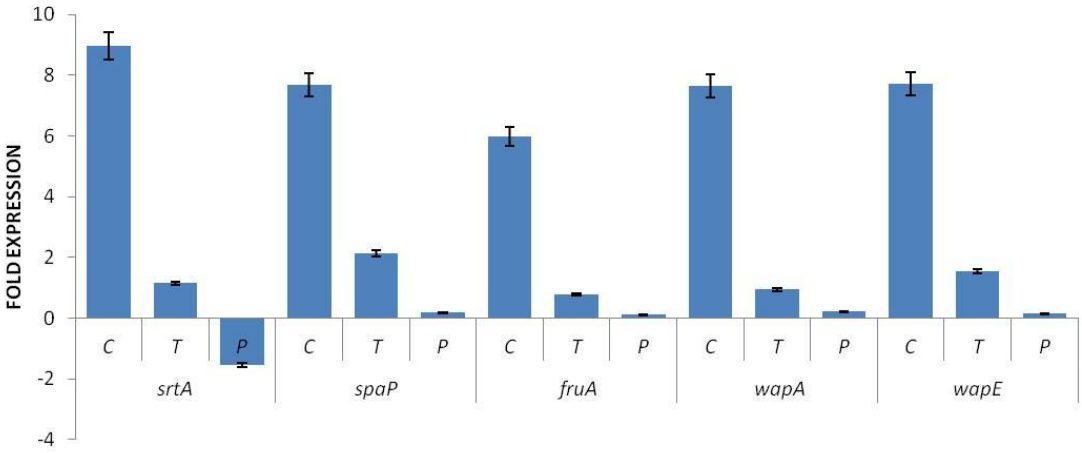

Fig.9: Graph showing the gene expression profiles of gene members under the treatment of the AgNPs mediated by *E.odoratum* leaf extract against *S.mutans.*All the values are average of triplicates and values are represented as value ±S.D. *** represents the significance of data remembered at P<0.05. C: Control (without AgNPs); T: Treatment (Synthesized AgNPs); P: positive control.

Discussion:

General health includes oral health. Globally, dental caries is the most prevalent chronic illness. This study sought to evaluate the antimicrobial activity of silver nanoparticles (AgNPs) synthesized by the green method using *Eupatorium odoratum* extract against oral pathogenic microorganisms, taking into account the significance of plaque control, complications of chemical agents, and the optimal antimicrobial efficacy of nanoparticles[15]. This investigation revealed that the bacteria with the lowest resistance to AgNPs generated using the green technique was*S. mutans*. Consistent with this discovery, copper nanoparticles produced utilizing the environmentally friendly approach and *Rhus punjabensis* extract demonstrated antibacterial qualities by Naz et al. (2018)[16]. Analogously, Dastjerdi *et al*. (2014) [17] demonstrated the antimicrobial properties of R. coriaria's aqueous extract against *S. mutans*.**Mostafa** et al (2014) [18]. validated the antibacterial activity of AgNPs synthesized by the green technique using olive tree leaves, which is consistent with the current findings about the green synthesis of AgNPs utilizing different plants. When compared to their chemical manufacture, Morinda pubescens is a suitable source for the green synthesis of AgNPs, as demonstrated by Zargar Mary et al. (2011) [19]. Furthermore, compared to chemical synthesis, the green production of AgNPs utilizing papaya tree leaves was less expensive and hazardous, according to Manish Dubey et al. (2010)[20]. A significant *S. mutans* surface protein called wall-associated protein A,

commonly known as AgIII, is encoded by the wapA gene [**21**]. According to research by Qian and Dao, *S. mutans* wapA inactivation reduces cell aggregation and adherence to smooth surfaces. The evidence points to a potential involvement for WapA in *S. mutans* colonisation of the tooth surface and subsequent development of dental biofilms. The main factor establishing *S. mutans* colonisation and deposition on tooth surfaces is its sucrose-dependent adherence inside the dental plaque. *WapA* is found to be significant to sucrose-dependent adhesion, however, is still debatable [**22**].*WapE* might well be involved in the adherence of this organism to the surface of the tooth and hence might aid in the production of dental plaque because wapE expression is elevated in *S. mutans* biofilm cells.

An enzyme called -D-fructosidase, which is encoded by the fruA gene, hydrolyzes fructans [23]. Polysaccharides called fructans are frequently produced by dental plaque microbes. Fructans are thought to act as energy storage polysaccharides because of their physical characteristics (big size and viscosity), which prevent them from diffusing out of the dental biofilm [24]. Therefore, by destroying fructans, FruA may increase cell survival during times of nutritional deprivation [25,26]. The degree and duration of the acid challenge at the tooth surface after sucrose exposure for S. mutans may be influenced by FruA. The absence of FruA in a *S. mutans* strain clearly does not change the cariogenic features of the strain in a rat model, despite the fact that FruA may be considered a possible virulence component. Against the two dental bacteria *Streptococcus mutans* and *Lactobacilli* sp., the combination of *Ficus benghalensis* prop root extract (FBPRE) and Ag_2O NPs shown outstanding antibacterial activity [27]. Similar results were observed in our study with significiant antibacterial activity against *S.mutans.*

CONCLUSION:

The present study has demonstrated that treatment with AgNPs on *S. mutans* caused a decrease in biofilm formation. This was also proved with real time PCR where all the five gene members *spaA, srtA, fruA, wapA* and *wapE* were under expressed providing potential antifungal nature of the synthesized AgNPs. This study offers proof of the impact of plant diversity on the structure of silver nanoparticle production. The generated Ag nanoparticles successfully interacted with biological molecules from plants, most likely phenolics, amides, or carbohydrates, as shown by the FTIR spectra. In TEM measurements, the produced NPs displayed two different morphologies: smaller spherical and bigger truncated octahedral forms. Finally, *S.mutans* was significantly sensitive to the synthesised AgNPs' antibacterial effects. Given that Eupatorium extract has been shown to have antimicrobial effects against

cariogenic germs, mouthwash, toothpaste, and dental floss may be formulated with Eupatorium extract to take advantage of these benefits.

REFERENCES:

1. Michiyo Matsumoto-Nakano, Role of Streptococcus mutans surface proteins for biofilm formation, Japanese Dental Science Review, Volume 54, Issue 1, 2018, Pages 22-29, ISSN 1882-7616, https://doi.org/10.1016/j.jdsr.2017.08.002.
2. Oho, T., and Nagata, E. (2019). DMBT1 involvement in the human aortic endothelial cell response to *Streptococcus mutans*. *Mole. Microbiol.* 34, 108–117. doi: 10.1111/omi.12257
3. Larson, M. R., Rajashankar, K. R., Crowley, P. J., Kelly, C., Mitchell, T. J., Brady, L. J., et al. (2011). Crystal structure of the C-terminal region of *Streptococcus mutans* antigen I/II and characterization of salivary agglutinin adherence domains. *J. Biol. Chem.* 286, 21657–21666. doi: 10.1074/jbc.M111.231100
4. Madsen, J., Mollenhauer, J., and Holmskov, U. (2010). Review: Gp-340/DMBT1 in mucosal innate immunity. *Innate Immun.* 16, 160–167. doi: 10.1177/1753425910368447
5. Lévesque CM, Voronejskaia E, Huang YC, Mair RW, Ellen RP, Cvitkovitch DG. Involvement of sortase anchoring of cell wall proteins in biofilm formation by *Streptococcus mutans.* Infect Immun 2005;73(6):3773-7. doi: 10.1128/IAI.73.6.3773-3777.2005. PMID: 15908410; PMCID: PMC1111851.
6. Elbeshehy E K F, Elazzazy A M, and Aggelis G. Silver nanoparticles synthesis mediated by new isolates of Bacillus spp., nanoparticle characterization and their activity against bean yellow mosaic virus and human pathogens. Front. Microbiol 2015; 6:453. doi: 10.3389/fmicb.2015. 00453.
7. Panda SK, LP Padhi and G Mohanty. Antibacterial activities and phytochemical analysis of *Cassia fistula* (Linn.) leaf. J. Adv. Pharmaceut. Technol Res 2011; 2: 62-67.
8. Masum M M I, Liu L, Yang M, Hossain M M, Siddiqa M M, Supty M E. Halotolerant bacteria belonging to operational group Bacillus amyloliquefaciens in biocontrol of the rice brown stripe pathogen Acidovorax oryzae. J. Appl. Microbiol 2018; doi: 10.1111/jam.14088.
9. Malla Sudhakar and B Venkata Raman. Bactericidal and Anti-biofilm Activity of Tannin Fractions Derived from *Azadirachta* against *Streptococcus mutans*. Asian Journal of Applied Sciences2020; 13: 132-143.
10. Ajdic D, W M McShan, R E McLaughlin, G Savic, J Chang, M B Carson, C Primeaux, R Tian, S Kenton, H Jia, S Lin, Y Qian, S Li, H Zhu, F Najar, H Lai, J White, B ARoe, and J J Ferretti. Genome sequence of *Streptococcus mutans* UA159, a cariogenic dental pathogen. Proc. Natl. Acad. Sci 2002. USA 99**:**14434-14439.
11. Paterson G K, and T J Mitchell. The biology of gram-positive sortase enzymes. Trends Microbiol 2004; 12**:**89-95.
12. Comfort D, and R T Clubb. A comparative genome analysis identifies distinct sorting pathways in gram-positive bacteria. Infect. Immun 2004; **72:**2710-2722.
13. Nicolas GG, Lavoie MC. *Streptococcus mutans* et les streptocoques buccaux dans la plaque dentaire. Can J Microbiol 2011;57(1):1-20. French. doi: 10.1139/w10-095. PMID: 21217792.
14. Mitchell T J. The pathogenesis of streptococcal infections: from tooth decay to meningitis. Nat. Rev. Microbiol. 2003; 1**:**219-230.
15. Nazemi Salman B, Mohammadi Gheidari M, Yazdi Nejad A, Zeighami H, Mohammadi A, Basir Shabestari S. Antimicrobial Activity of Silver Nanoparticles Synthesized by the Green Method Using *Rhus coriaria L*. Extract Against Oral Pathogenic Microorganisms. Med J Islam Repub Iran. 2022 Dec 15;36:154. doi: 10.47176/mjiri.36.154. PMID: 36654848; PMCID: PMC9832934.
16. Naz S, Tabassum S, Freitas Fernandes, Mujahid M, Zia M, Blanco EJ. Anticancer and antibacterial potential of Rhus punjabensis and CuO nanoparticles. *Nat Product Res.* 2018:1–6.
17. Vahid Dastjerdi E, Sarmast Z, Abdolazimi Z, Mahboubi A, Amdjadi P, Kamalinejad M. Effect of Rhus coriaria L. water extract on five common oral bacteria and bacterial biofilm formation on orthodontic wire . *Iran J Microbiol* . 2014 ;6(4):269–275.
18. Mostafa MH, Eman K, Ismail H, El-Baghdady KZ, Mohamed D. Green synthesis of silver nanoparticles using olive leaf extract and its antibacterial activity. *Arab J Chem.* 2014:1131–1139.

19. Zargar M, Abdul Hamid, Abu Bakar, Shamsudin MN, Shameli K, Jahanshiri F. et al. Green Synthesis and Antibacterial Effect of Silver Nanoparticles Using Vitex Negundo L. *Molecules.* 2011;16:6667–6676.
20. Dubey SH, Sillan P. Green synthesis and characterizations of silver and gold nanoparticles using leaf extract of Rosa rugosa. *Colloids and Surfaces A: Physicochemical and Engineering Aspects.* 2010;364(1-3):34–41.
21. Anita Staroń & Olga Długosz Antimicrobial properties of nanoparticles in the context of advantages and potential risks of their use, Journal of Environmental Science and Health 2001; 56:6, 680-693, DOI: 10.1080/10934529.2021.1917936
22. Loo Y Y, Chieng B W, Nishibuchi M, and Radu S. Synthesis of silver nanoparticles by using tea leaf extract from *Camellia sinensis*. *Int. J. Nanomed.* 2012; 7, 4263–4267. doi: 10.2147/IJN.S33344
23. Selvam K, Sudhakar C, Govarthanan M, Thiyagarajan P, Sengottaiyan A, Senthilkumar B, et al. Eco-friendly biosynthesis and characterization of silver nanoparticles using *Tinospora cordifolia* (Thunb.) Miers and evaluate its antibacterial, antioxidant potential. J. Radiat. Res. Appl. Sci 2017; 10, 6–12. doi: 10.1016/j.jrras.2016.02.005
24. Garcia CC, Talarico L, Almeida N, Colombers S, Duschatzky C, Damonte EB. Virucidal activity of essential oils from aromatic plants of San Luis, Argentina. Phytotherapy Research 2003; 17: 1073-1075.
25. Kunle O, Okogun J, Egamana E, Emojevwe E, Shok M. Antimicrobial activity of various extracts and carvacrol from Lippia multiflora leaf extract. Phytomedicine 2003; 10, 59-61.
26. Manikandan V, Velmurugan P, Park JH, Chang WS, Park YJ, Jayanthi P, Cho M, Oh BT. Green synthesis of silver oxide nanoparticles and its antibacterial activity against dental pathogens. Biotech 2017;7(1):72. doi: 10.1007/s13205-017-0670-4. Epub 2017 Apr 27. PMID: 28452017; PMCID: PMC5428112.
27. Lucchese, A. (2017). *Streptococcus mutans* antigen I/II and autoimmunity in cardiovascular diseases. *Autoimmun. Rev.* 16, 456–460. doi: 10.1016/j.autrev.2017.03.009
28. Samy, M. A., Abbassy, M. A., Hafez, E. E., Rabea, E. I., & Aseel, D. G. (2019). Biosynthesis and Characterization of Silver Nanoparticles Produced by Plant Extracts and Its Antimicrobial Activity. South Asian Journal of Research in Microbiology, 3(1), 1–14. https://doi.org/10.9734/sajrm/2019/v3i130077
29. Uba , B. O., Okoye , E. L., Anyichie, J. C., Dokubo , C. U., & Ugwuoji , E. T. (2024). Synthesis, Characterization and Application of Biogenic Silver Nanoparticles as Antibacterial and Antifungal Agents. Journal of Advances in Microbiology, 24(3), 65–78. https://doi.org/10.9734/jamb/2024/v24i3809
30. Khalil MM, Ismail EH, El-Baghdady KZ, Mohamed D. Green synthesis of silver nanoparticles using olive leaf extract and its antibacterial activity. Arabian Journal of chemistry. 2014 Dec 1;7(6):1131-9.

UNDER PEER REVIEW